ChemComm

Accepted Manuscript

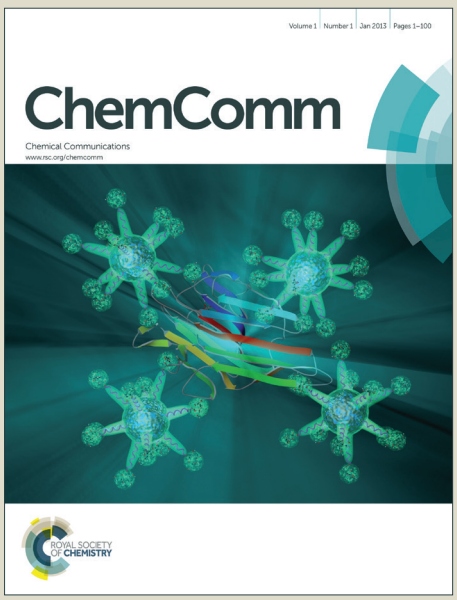

ROYAL SOCIETY OF CHEMISTRY

www.rsc.org/chemcomm

ChemComm

COMMUNICATION

Interfacial Ordering of Thermotropic Liquid Crystals Triggered by the Secondary Structures of Oligopeptides

Received 00th January 20xx,
Accepted 00th January 20xx

DOI: 10.1039/x0xx00000x

www.rsc.org/

Xiaoguang Wang,[‡a] Pei Yang,[‡b] Frederic Mondiot,[a] Yaoxin Li,[b] Daniel S. Miller,[a] Zhan Chen*[b] and Nicholas L. Abbott*[a]

We report that assemblies formed by eight oligopeptides at phospholipid-decorated interfaces of thermotropic liquid crystals (LCs) trigger changes in ordering of the LCs that are dependent on the secondary structures of the oligopeptides (as characterized *in situ* using infrared-visible sum-frequency spectroscopy).

The functional properties of oligopeptides and proteins at interfaces depend strongly on their secondary structures and higher level organization.[1] This coupling of structure and function is particularly evident at biological interfaces such as cell membranes, and is increasingly important in the design of synthetic materials that are programmed to direct or sense a biological response.[2, 3]

This Communication describes the finding that the secondary structures assumed by oligopeptides at phospholipid-decorated interfaces of thermotropic liquid crystals (LCs; fluid phases within which the constituent molecules exhibit long-range orientational order) can trigger distinct ordering patterns in the LCs. It builds broadly from the observation that interfacial molecular assemblies formed at aqueous—LC interfaces can generate changes in ordering that propagate deep into the LCs, and thus can be transduced optically, with micrometer-scale resolution, by using polarized light (PL) microscopy.[4] More specifically, in past studies of assemblies formed by proteins and phospholipids at aqueous interfaces of thermotropic LCs, we observed protein—protein interactions to give rise to a range of interfacial assemblies that possessed distinct micrometer-scale morphologies.[4a,5] While such biomolecular assemblies have been observed by us and others,[4b, 6] little is understood about the factors that control their formation or coupling to the LC.

Herein we explore the question of whether the secondary structures of oligopeptides adsorbed at interfaces between thermotropic LCs and aqueous phases, including phospholipid-decorated interfaces that recapitulate some characteristics of biological membranes (*e.g.*, lateral mobility), influence the ordering of LCs. In these studies, we used eight antimicrobial oligopeptides because past investigations document their secondary structures in bulk solutions and within lipid bilayers.[7] Infrared-visible sum-frequency generation (SFG) vibrational spectroscopy is used to characterize the secondary structures of the oligopeptides at the LC interfaces.

The initial experiments reported below employed L-α-dilaurylphophatidylcholine (DLPC)-decorated interfaces of micrometer-thick films of nematic 4-cyano-4'-pentylbiphenyl (5CB). The films were submerged in aqueous phosphate buffered saline (PBS), as shown in Fig. 1A (see ESI† for details). Initially, we measured the LC films to exhibit a uniformly dark optical appearance, consistent with homeotropic (perpendicular) anchoring of nematic 5CB at the DLPC-laden aqueous interface of the LC (see Fig. S1, ESI†). Past studies have established that steric interactions between the acyl tails of lipids and mesogens cause LCs to adopt homeotropic orientations.[4-6] Next, we incubated the LCs against PBS containing either Cecropin P1 (SWLSKTAKKLENSAKKRISEGIAIAIQGGRRC) or Lactoferricin B (FKCRRWQWRMKKLGAPSITCVRRAF). As noted above, these oligopeptides were selected because they have been reported previously to adopt distinct secondary structures in bulk aqueous solutions - Cecropin P1 is largely random coil[7a] and Lactoferricin B adopts a structure rich in β-sheets and β-turns.[7c] Fig. 1B-G shows the dynamic optical response of the LC to adsorption of Cecropin P1. Ten minutes after the addition of the oligopeptide, micrometer-sized domains with an ellipsoidal shape and a bright optical appearance (corresponding to regions of LCs with a tilted alignment) nucleated at the interface. The domains were laterally mobile, and over the subsequent 40 mins (Fig. 1D-G), they grew and coalesced,

[a] Department of Chemical and Biological Engineering, University of Wisconsin-Madison, 1415 Engineering Drive, Madison, WI 53706 (USA). Email: abbott@engr.wisc.edu
[b] Department of Chemistry, University of Michigan, 930 North University Avenue, Ann Arbor, MI 48109 (USA). Email: zhanc@umich.edu

† Electronic Supplementary Information (ESI) available: Materials and Methods, quantification of coverage of lipid monolayer at aqueous—LC interfaces, fluorescence microscopy of optical response of LCs to adsorption of oligopeptides, influence of LC elasticity on formation of optical domains by oligopeptides at LC interfaces, fractal dimensions analysis, and SFG characterization. See DOI: 10.1039/x0xx00000x

‡ These authors contribute equally to this work.

Table 1. Summary of secondary structure of oligopeptides

oligopeptide	bulk solution	lipid bilayer	aqueous—LC interface (wavenumber, cm^{-1})
Cecropin P1	RC [a, 7a]	αH [b, 7b]	αH(1658)
Lactoferricin B	βS+βT [c, 7c]	βS+βT [d, 7d]	βS(1635) + βT(1663)
MSI-594	RC [e, 7e]	αH [f, 7f]	αH(1658)
MSI-78	RC [e, 7e]	αH [g, 7g]	αH(1658)
Tachyplesin I	βS+βT [h, 7h]	βS+βT [i, 7i]	not conclusive
Protegrin 1	βS+βT [j, 7j]	βS+βT [k, 7k]	no signal
Alamethicin	αH [l, 7l]	αH+3_{10}H [m, 7m]	3_{10}H(1642) + αH(1658)
CecropinA-Melittin	βS [n, 7n]	αH [o, 7n]	αH(1655) + βT(1663)

αH: α-helix; RC: random coil; 3_{10}H: 3_{10}-helix; βS: β-sheet; βT: β-turn. [a] By nuclear magnetic resonance (NMR) and circular dichroism (CD) in 30% propanol aqueous solution. [b] By attenuated total reflectance Fourier-transform infrared (ATR-FTIR) spectroscopy. [c] By NMR in 90% H2O/10% D2O. [d] By ATR-FTIR. [e] By CD in Tris buffer. [f] By CD and NMR. [g] By NMR. [h] By NMR in trifluoroacetic acid buffer aqueous solution. [i] By SFG. [j] By NMR in phosphate buffer solution. [k] By NMR. [l] By NMR. [m] By SFG. [n] By CD in phosphate buffer solution. [o] By CD.

resulting in ellipsoidal domains with lateral sizes of tens of micrometers. After approximately 1 hour, the rate of change of appearance of the LC slowed substantially. At this point, the bright domains were "pear-shaped". In contrast, within 10-20 mins of addition of the Lactoferricin B to the aqueous phase, LC domains with a dendritic shape formed across the LC interface (Fig. 1I). Over the subsequent 40 mins (Fig. 1J-M), the domains grew and coalesced in a highly anisotropic fashion, with growth being fastest along the long axis of the domains. We emphasize that the addition of oligopeptides did not initiate domain growth when the 5CB was heated into the isotropic phase, revealing that the supramolecular (nematic) ordering of the LC plays a key role in driving the formation and growth of the interfacial domains of oligopeptides (see below and Fig. S6 and S7 in ESI†).

The results shown in Fig. 1 are consistent with changes in ordering of the LCs that are triggered by the adsorption, penetration and assembly of oligopeptides at the DLPC-decorated LC interfaces (Fig. 1A). In contrast to phospholipids, which cause homeotropic anchoring of LCs,[4a] oligopeptides or proteins cause tilted anchoring.[4a,5] Therefore, we assign the bright optical domains in Fig. 1 to be oligopeptide-rich regions whereas the dark regions are interpreted to be rich in DLPC. This assignment was confirmed by fluorescence microscopy using Cecropin P1/Texas Red-labelled lipids (see ESI†).[4a,5] Here we emphasize that the response of the LC to the adsorption of the oligopeptides involves lateral reorganization of the lipids at the LC interface (Fig. 1A and Fig. S5B in ESI†). Because the two oligopeptides used in the experiments shown in Fig. 1 possess distinct secondary structures in bulk solutions, these results lead us to speculate that the shapes of the oligopeptide-rich domains may be influenced by the secondary structure of the oligopeptides adsorbed at the LC interfaces.

To test further this hypothesis, we performed measurements with six additional oligopeptides, as shown in Fig. 2 and Table 1. We observed four broad behaviours. First, ellipsoidal domains similar to those formed with Cecropin P1

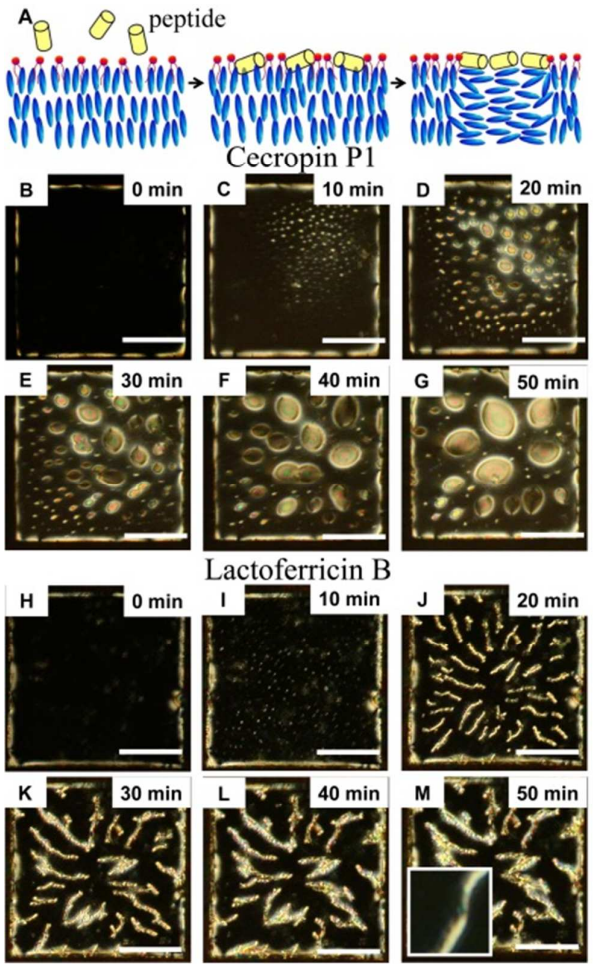

Fig. 1 (A) Schematic illustration of adsorption of oligopeptides at DLPC-laden aqueous—LC interface. Optical micrographs (crossed polarizers) of the dynamic response of the LC to the adsorption of (B-G) Cecropin P1 or (H-M) Lactoferricin B at a DLPC-laden aqueous—5CB interface. An enlarged region of (M) is shown in the inset. The times at which the micrographs were obtained following injection of oligopeptides into the aqueous solution are indicated. The final concentration of oligopeptides was 2 μM. Scale bars: 100 μm. Corresponding movies are available in the ESI†.

were observed upon adsorption of MSI-594 (GIGKFLKKAKKGI-GAVLKVLTTGL) or MSI-78 (GIGKFLKKAKKFGKAFVKILKK), as shown in Fig. 2A-D. Past studies have reported MSI-594 and MSI-78 to be predominantly random coils in bulk solutions,[7e] similar to Cecropin P1. Second, a network of elongated domains similar to Lactoferricin B was observed with Tachyplesin I (KWCFRVCYRGICYRRCR) or Protegrin 1 (RGGRLCYCRRRFCVCVGR), as shown in Fig. 2E-H. Previous studies have reported Tachyplesin I and Protegrin 1 to form β-sheets and β-turns in bulk solutions,[7h,j] similar to Lactoferricin B.[7c] Third, Alamethicin (APAAAAQAVAGLAPVAAEQF), which adopts an α-helical conformation in bulk solution,[7l] generated compact but irregular-shaped (non-ellipsoidal) domains, as shown in Fig. 2I and J. Fourth, Cecropin A-Melittin hybrid peptide (KWKLFKKIGIGAVLKVLTTGLPALIS), which forms β-sheets in bulk solutions,[7n] generated elongated and dendritic domains across the LC interface, as shown in Fig. 2K and L. Here we comment that the LC domain shapes generated by

Alamethicin and Cecropin A-Melittin have features that are distinct from those generated by other peptides reported in this Communication (Fig. 2A-2H or Fig. 1), a point that we return to below.

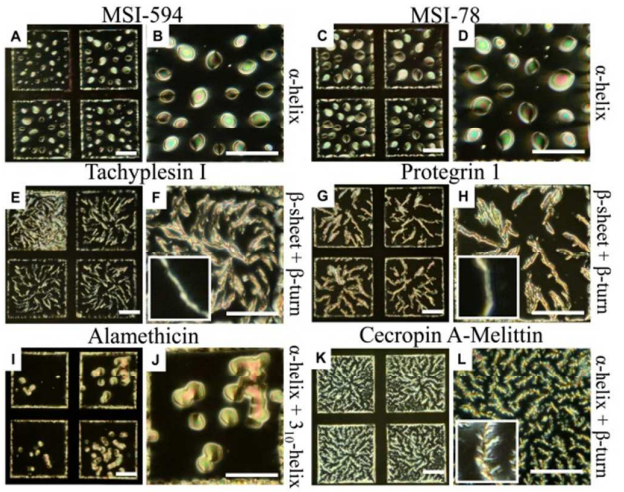

Fig. 2 PL micrographs (crossed polarizers) of the optical response of the LCs to the adsorption of oligopeptides having different secondary structures at the DLPC-laden aqueous—LC interfaces: (A, B) MSI-594; (C, D) MSI-78; (E, F) Tachyplesin I; (G, H) Protegrin 1; (I, J) Alamethicin; (K, L) Cecropin A-Melittin hybrid peptide. Enlarged regions of (F), (H) and (L) are shown in the insets. All the images are captured at 1 hour after addition of oligopeptides. The secondary structures measured by SFG are listed to the right of the micrographs except for Protegrin I, the secondary structure of which is based on Ref 7*k*. The final concentration of each oligopeptide was 2 μM. Scale bars: 100 μm.

Next, we sought to characterize the secondary structures of the oligopeptides at the LC interfaces to rigorously test the hypothesis that the shape of the LC domain is dependent on the oligopeptide secondary structure. As detailed in the ESI†, a polymer network-stabilized LC film was used for these SFG measurements (see ESI† for details of both SFG and sample preparation). We obtained SFG spectra of oligopeptides at both DLPC-free and DLPC-decorated LC interfaces to explore the effect of interfacial environments on the conformational states of the oligopeptides, and in particular, the extent to which the LC provides an interfacial environment that is similar to a lipid monolayer. Spectroscopic characterization of aqueous—LC interfaces has not been reported previously, but past studies using SFG have established that the position of the amide I band (which arises mainly from C=O stretching vibration) changes with the conformational state of peptides/proteins.[8] The SFG spectra of oligopeptides adsorbed at aqueous—LC interfaces are shown in Fig. 3 (see Table 1 for assignments of the peak positions). Unless otherwise stated, the amide I positions measured for the oligopeptides adsorbed at the DLPC-decorated LCs were identical to those shown in Fig. 3 and Table 1 (see ESI†).

First, for Cecropin P1, we measured an amide I peak at ~ 1658 cm^{-1} (Fig. 3A), which is consistent with an α-helical secondary structure. A similar signal was observed for MSI-594 and MSI-78 (Fig. 3B and C), which reveals the secondary structures of these LC-adsorbed oligopeptides to be similar to those found in lipid bilayers.[7b,f,g] These results lead us to propose that oligopeptides rich in α-helical content at LC interfaces generate ellipsoidal domains in the LCs, as shown in Fig. 1G and 2A-D. We comment here that the peak at ~1610 cm^{-1} in Fig. 3C, D and F is due to the polymer network used to stabilize the LC film (see ESI† for details).

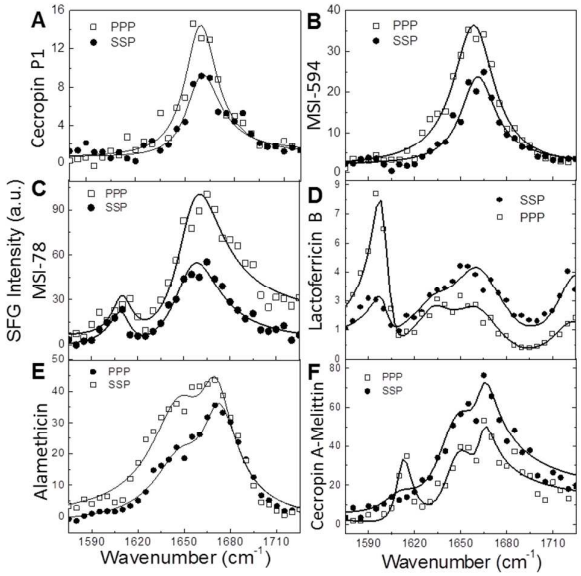

Fig. 3 SFG spectra collected from aqueous—LC interfaces with adsorbed oligopeptides: (A) Cecropin P1; (B) MSI-594; (C) MSI-78; (D) Lactoferricin B; (E) Alamethicin; (F) Cecropin A-Melittin hybrid peptide. Dots: experimental data; Lines: fit to a Lorentzian line-shape model. See ESI† for additional information regarding fitting of the spectra.

Second, previous studies have shown that Lactoferricin B, Tachyplesin I and Protegrin 1, which triggered formation of elongated domains at aqueous—LC interfaces (Fig. 1M and Fig. 2E-H), adopt β-sheet and β-turn secondary structures in bulk solutions and lipid bilayers.[7c,d,h-k] Although the SFG signals were weak (see below for additional comments on this point), for Lactoferricin B, we observed amide I peaks at ~ 1635 cm^{-1} and ~ 1663 cm^{-1}, corresponding to β-sheet/β-turn content, respectively (Fig. 3D; see ESI† for discussion of line-shape fitting to the experimental data). For Protegrin 1, no SFG signal was obtained from 10 independent measurements. For Tachyplesin I, a weak signal was measured. Interestingly, although the Tachyplesin I signal was noisy, by using parameters obtained for the fit of Lactoferricin B, we were able to describe the Tachyplesin data in a manner consistent with β-sheet/β-turn content (see ESI† for details). Overall, these results provide evidence that oligopeptides that generate elongated LC domains contain β-sheet/β-turn content. In addition, the weak SFG signal indicates that either these oligopeptides were adsorbed with a distribution of orientations that generate a weak signal or the hyperpolarizability of the β-sheet structure is low.

Third, as noted above, the LC domains induced by Alamethicin (compact and irregular-shaped orientational domains; Fig. 2I and J) or Cecropin A-Melittin hybrid peptides (dendritic domains; Fig. 2K and L) were different from those induced by oligopeptides with either α-helix or β-sheet/β-turn structures.[7l,n] Therefore, we used SFG to determine if Alamethicin and Cecropin A-Melittin hybrid peptides adopted

secondary structures at the LC interface that were not, in fact, α-helix or β-sheet/β-turn, as suggested by the ordering of the LC. Significantly, in SFG spectra, we observed amide I peaks at ~1642 cm^{-1} and ~1658 cm^{-1} for Alamethicin (Fig. 3E) and peaks at ~1655 cm^{-1} and 1663 cm^{-1} for Cecropin A-Melittin hybrid peptide (Fig. 3F), corresponding to 3_{10}-helix/α-helix content (for Alamethicin[7m]) and α-helix/β-turn content (for Cecropin A-Melittin hybrid peptide), respectively. This correspondence between the SFG signal and orientational ordering of the LC, thus provides further support for the hypothesis that the shapes of the optical domains at the LC interface are dependent on the secondary structures of the oligopeptides. We note here also that the secondary structure of the Cecropin A-Melittin hybrid peptide at the LC interface is distinct from that found previously either in bulk solution or in a lipid bilayer.[7n]

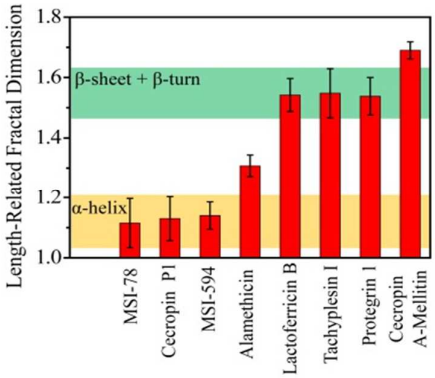

Fig. 4 Influence of oligopeptide secondary structure on the fractal dimensions of optical domains formed by various oligopeptides at aqueous—LC interfaces.

Past studies of the aggregation of oligopeptides in bulk aqueous solution have not found a correlation between secondary structure and aggregate morphology.[9] We emphasize, however, that our study is conducted at the aqueous—LC interface, and that our results establish that the ordering of the LC influences the oligopeptide domain formation. To quantify the shapes of the oligopeptides assemblies, we calculated the fractal dimension (*D*) of the domains (see ESI† for details). The fractal dimensions shown in Fig. 4 correlate strongly with oligopeptide secondary structure. This result hints that measurements of *D* might provide a facile way to infer the secondary structure of interfacial oligopeptides (α-helix versus β-sheet/β-turn). Our results also lead to a number of other interesting insights. Specifically, our results reveal that the supramolecular ordering of the LC drives the oligopeptide-rich domain formation – in the absence of nematic ordering of the LC, domain formation is not observed (see Fig. S6 and S7 and associated ESI† text). In addition, we note that the above-described formation of oligopeptide-rich domains leads to the lateral reorganization of phospholipids on the LC interface, which in turn triggers a change in the ordering and optical appearance of the LC. More broadly, these results hint at new interfacial designs of LC materials that can report changes in the interfacial conformational states of oligopeptides without requiring complex or expensive equipment (*e.g.*, ATR-FTIR,[10] CD,[10] NMR,[10] Raman spectroscopy,[10] and SFG[8]). Finally, our results suggest that LC interfaces might offer the basis of mimics of biological membranes from which biophysical insights may be gained in future studies (*e.g.*, interfacial organization of antimicrobial peptides).

We acknowledge support for this work from the ARO (W911NF-11-1-0251 and W911NF-14-1-0140), and facilities supported by NSF (Wisconsin MRSEC, DMR-1121288).

Notes and references

1 (*a*) X. Zhao, F. Pan, H. Xu, M. Yaseen, H. Shan, C. A. E. Hauser, S. Zhang, J. Lu, *Chem. Soc. Rev.*, 2010, **39**, 3480; (*b*) A. V. Pinheiro, D. Han, W. M. Shih, H. Yan, *Nat. Nanotechnol.*, 2011, **6**, 763.

2 (*a*) V. Teixeira, M. Feio, M. Bastos, M. *Prog. Lipid Res.*, 2012, **51**, 149; (*b*) A. Ciaccafava, P. Infossi, M. Ilbert, M. Guiral, S. Lecomte, M. T. Giudici-Orticoni, E. Lojou, *Angew. Chem. Int. Ed.,* 2012, **51**, 953.

3 (*a*) Y. Liu, T. L. Ogorzalek, P. Yang, M. M. Schroeder, E. N. G. Marsh, Z. Chen, *J. Am. Chem. Soc.,* 2013, **135**, 12660; (*b*) S. Segman, M. Lee, V. Vaiser, S. H. Gellman, H. Rapaport, *Angew. Chem. Int. Ed.,* 2010, **49**, 716.

4 (*a*) J. M. Brake, M. K. Daschner, Y. Y. Luk, N. L. Abbott, *Science,* 2003, **302**, 2094; (*b*) A. D. Price, D. K. Schwartz, *J. Am. Chem. Soc.,* 2008, **130**, 8188.

5 M. D. de Tercero, N. L. Abbott, *Chem. Eng. Comm.,* 2009, **196**, 234.

6 (*a*) P. S. Noonan, R. H. Roberts, D. K. Schwartz, *J. Am. Chem. Soc.,* 2013, **135**, 5183; (*b*) C. Y. Chang, C. H. Chen, *Chem. Commun.,* 2014, **50**, 12162; (*c*) Q. Z. Hu, C. H. Jang, *Analyst*, 2012, **137**, 567.

7 (*a*) J. R. Uzarski, A. Tannous, J. R. Morris, C. M. Mello, *Colloids Surf., B,* 2008, **67**, 157; (*b*) E. Gazit, I. R. Miller, P. C. Biggin, M. S. P. Sansom, Y. Shai, *J. Mol. Biol.,* 1996, **258**, 860; (*c*) P. M. Hwang, N. Zhou, X. Shan, C. H. Arrowsmith, H. J. Vogel, *Biochemistry,* 1998, **37**, 4288; (*d*) M. Arseneault, S. Bedard, M. Boulet-Audet, M. Pezolet, *Langmuir*, 2010, **26**, 3468; (*e*) A. Ramamoorthy, S. Thennarasu, D. Lee, A. Tan, L. Maloy, *Biochem. J.*, 2006, **91**, 206; (*f*) P. N. Domadia, A. Bhunia, A. Ramamoorthy, S. Bhattacharjya, *J. Am. Chem. Soc.*, 2010, **132**, 18417; (*g*) K. J. Hallock, D. Lee, A. Ramamoorthy, *Biophys. J.*, 2003, **84**, 3052; (*h*) A. Laederach, A. H. Andreotti, D. B. Fulton, *Biochemistry*, 2002, **41**, 12359; (*i*) A. P. Boughton, K. Nguyen, I. Andricioaei, Z. Chen, *Langmuir*, 2011, **27**, 14343; (*j*) R. L. Fahrner, T. Dieckmann, S. S. L. Harwig, R. I. Lehrer, D. Eisenberg, J. Feigon, *Chem. Biol.,* 1996, **3**, 543; (*k*) S. Yamaguchi, T. Hong, A. Waring, R. I. Lehrer, M. Hong, *Biochemistry,* 2002, **41**, 9852; (*l*) U. Banerjee, F. P. Tsui, T. N. Balasubramanian, G. R. Marshall, S. I. Chan, *J. Mol. Biol.*, 1983, **165**, 757; (*m*) P. Yang, F. G. Wu, Z. Chen, *J. Phys. Chem. C,* 2013, **117**, 3358; (*n*) F. Abrunhosa, S. Faria, P. Gomes, I. Tomaz, J. C. Pessoa, D. Andreu, M. Bastos, *J. Phys. Chem. B,* 2005, **109**, 17311.

8 (*a*) X. Chen, M. L. Clarke, J. Wang, Z. Chen, *Int. J. Mod. Phys. B,* 2005, **19**, 691; (*b*) G. A. Somorjal, H. Frel, J. Y. Park, *J. Am. Chem. Soc.*, 2009, **131**, 16589; (*c*) S. Y. Jung, S. M. Lim, F. Albertorio, G. Kim, M. C. Gurau, R. D. Yang, M. A. Holden, P. S. Cremer, *J. Am. Chem. Soc.,* 2003, **125**, 12782; (*d*) L. Fu, E. C. Y. Yan, *J. Am. Chem. Soc.,* 2011, **133**, 8094; (*e*) T. Weidner, D. G. Castner *Phys. Chem. Chem. Phys.,* 2013, **15**, 12516; (*f*) S. J. Roeters, C. N. van Dijk, A. Torres-Knoop, E. H. G. Backus, R. K. Campen, M. Bonn, S. Woutersen, *J. Phys. Chem. A,* 2013, **117**, 6311; (*g*) B. O. Leung, Z. Yang, S. S. H. Wu, K. C. Chou, *Langmuir*, 2012, **28**, 5724.

9 T. R. Jahn, S. E. Radford, *Arch. Biochem. Biophys.*, 2008, **469**, 100.

10 H. J. Dyson, P. E. Wright, *Annu. Rev. Biophys. Chem.,* 1991, **20**, 519.